

## Case Study: Wear in Supersonic Nozzle of Tip Lance in Vallourec Brazil Steelmaking

Fabrcio Silveira Garajau<sup>1</sup>; Marcelo de Souza Lima Guerra<sup>1</sup>, Breno Totti Maia<sup>1</sup>, Paulo Roberto Cetlin<sup>2</sup>, Dione Araújo Moreira<sup>3</sup>.

<sup>1</sup> Lumar Metals Ltda.  
Rod. MG 232, km 09, N° 100, Santana do Paraíso/MG, Brazil, 35.167-000

<sup>2</sup> UFMG  
Boulevard Antônio Carlos, 6627 Fields Pampulha, Belo Horizonte/MG, Brazil, 31270-901

<sup>3</sup> Vallourec Brazil S.A.  
Avenue Olinto Meireles, 65, Belo Horizonte/MG, Brazil, 30640-010

Keywords: Tip lance, supersonic nozzle, wear, CFD simulation.

### ABSTRACT

The supersonic nozzle wear has been the biggest limitation in life of tip lance in Vallourec Brazil steelmaking, with approach 600 heats. Vallourec use in lances the Slagless cartridge, developed by Lumar Metals Ltd., which has potential to operate more than 1200 heats. To achieve it is necessary eliminating the wear in outlet nozzle. In this work will be presented the methodology and results of a failure analysis made in some samples from a tip with wear in supersonic nozzle, aiming correlate the metallography results with CFD simulations of blowing process, for characterization the wear mechanism and the resizing the nozzle. The main results are characterizing the wear mechanism and propose a methodology for resizing to avoid the wear.

### 1. INTRODUCTION

The oxygen blowing is the main stage in steelmaking refining with BOF (Basic Oxygen Furnace) converters. The blowing is calculating for specifics conditions, for example, oxygen flow rate and back pressure, height bath-lance, etc. Oxygen lance is the equipment used for supplying the oxygen necessary for decarburization reactions, through the supersonics nozzles located at lance tip face. This tip is commonly making in high purity copper, which can be casted, forged or centrifuged. The copper is a low melting point (approach 1085 °C), but is an excellent thermal conductor and when water cooled, provides adequate thermal extraction to maintain the face tip with temperatures below 300 °C <sup>(1)</sup>.

Figure 1 is showing a schematic drawing section of tip lance used in Vallourec Brazil converters, which has the capacity of 80t, where can be seen the supersonic nozzles, the inlet and outlet water cooling and the main oxygen inlet.

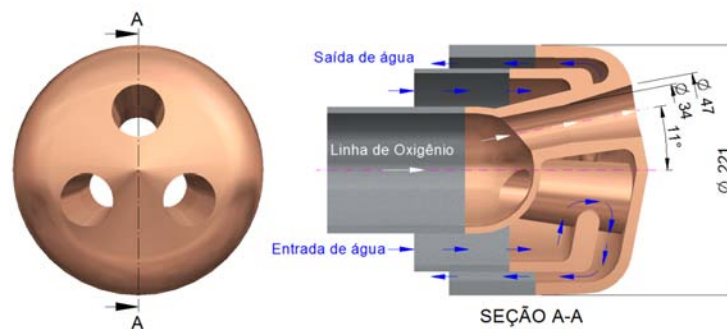


Figure 1 - Schematic drawing of tip lance used in Vallourec Brazil.

This tip works exposed in an aggressive environment immersed in the emulsion (melting-gas-slag) with high temperatures provide by exothermic chemical reactions. The reaction that occurs closer tip is the post combustion, as shown in Figure 2, which corresponds to the oxidation of CO from the decarburization of the metallic bath (reactions of O<sub>2</sub> injected with bath elements) with jet ends of O<sub>2</sub>, forming carbon dioxide (CO<sub>2</sub>).

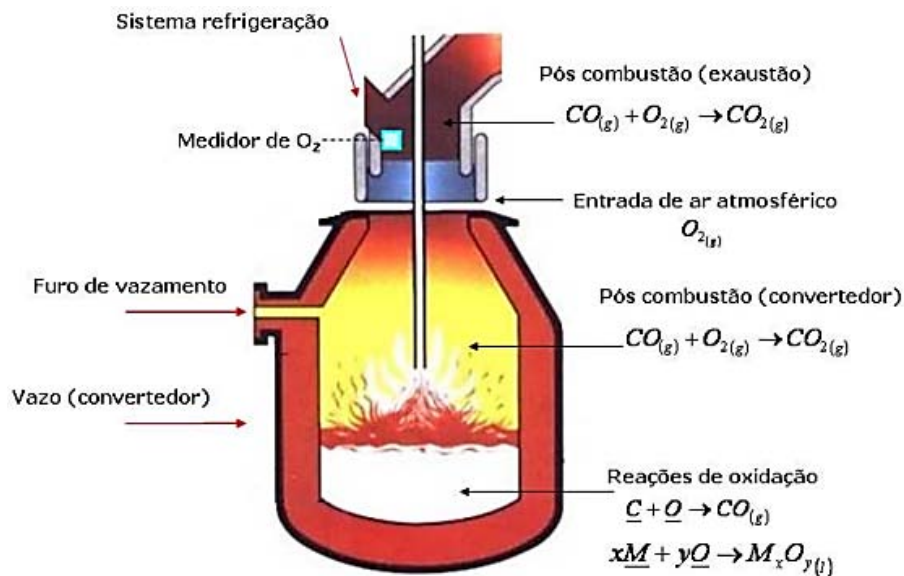


Figure 2: Schematic drawing of chemical reactions which occurs in BOF steelmaking refine <sup>(2)</sup>.

As the oxygen flow is compressible fluid flow with supersonics velocities, the Mach number dimensionless (M) is an important parameter to analysis, which correlations flow speed (v) with speed of sound (a), through equations 1 and 2 <sup>(3)</sup>:

$$M \equiv \frac{v}{a} \quad (1)$$

$$a = \sqrt{kRT} \quad (2)$$

Where: k - Reasons for specific heats; R - Ideal gas constant; T - Temperature.

Analyzing the Mach number of the supersonic jet can be characterized by the flow profile at the outlet of the nozzle. For a flow rate with  $M > 1$  and outlet pressure more than environment pressure ( $P_s > P_a$ ) the nozzle is characterized with under expanded, schematically showing in Figure 3a. In this case the nozzle has a reason of areas less than ideal, so that is a sufficient expansion for an ideal expansion condition. The remainder of the expansion will occur outside the nozzle and normal shock wave are replaced for an oblique shock wave, begin at the edge. <sup>(4)</sup>

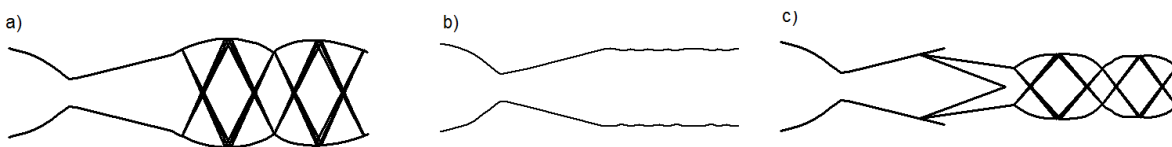


Figure 3: Nozzle characteristic types: a) under expanded, b) ideal expanded c) over expanded.

When the outlet pressure is equal the environment pressure ( $P_s = P_a$ ) don't occur the normal shock wave inside the nozzle and it reaches an operation regime called ideal expanded (Figure 3b). In flow with  $M > 1$  and outlet pressure more than environment pressure ( $P_s < P_a$ ), the nozzle is called over expanded, it's show in Figure 3c <sup>(5)</sup>.

Bad design of these nozzles has direct influence on the time and efficiency of process; also commonly result in premature outlet wear and the tip is put out of operation. These are important operational parameters for calculate the nozzles: m' (flow rate), P<sub>0</sub> (back pressure), T<sub>a</sub> (environment temperature) e P<sub>a</sub> (environment pressure). If these parameters are different of the

project specification, the nozzle can fast wear <sup>(6)</sup>. In Figure 4 is presented two images for compare between a new and old tip (after 600 heats). Understand the nozzle wear and present a methodology to solve this failure are the main goals of this job. To achieve it will be made a metallography of the failed area and the CFD to study the fluid dynamics of the phenomena.



Figure 4: a) New tip; and b) Same tip after 600 heats, displaying nozzle wear.

## 2. METHODS AND MATERIALS

### 2.1. Metallography analysis

It was used some samples achieved in a tip putted out from operation with the failure of nozzle wear. The samples wear was cutting in three different parts regions (Figure 5) for metallographic analysis, to possibility verify the microstructure variations caused by wear.

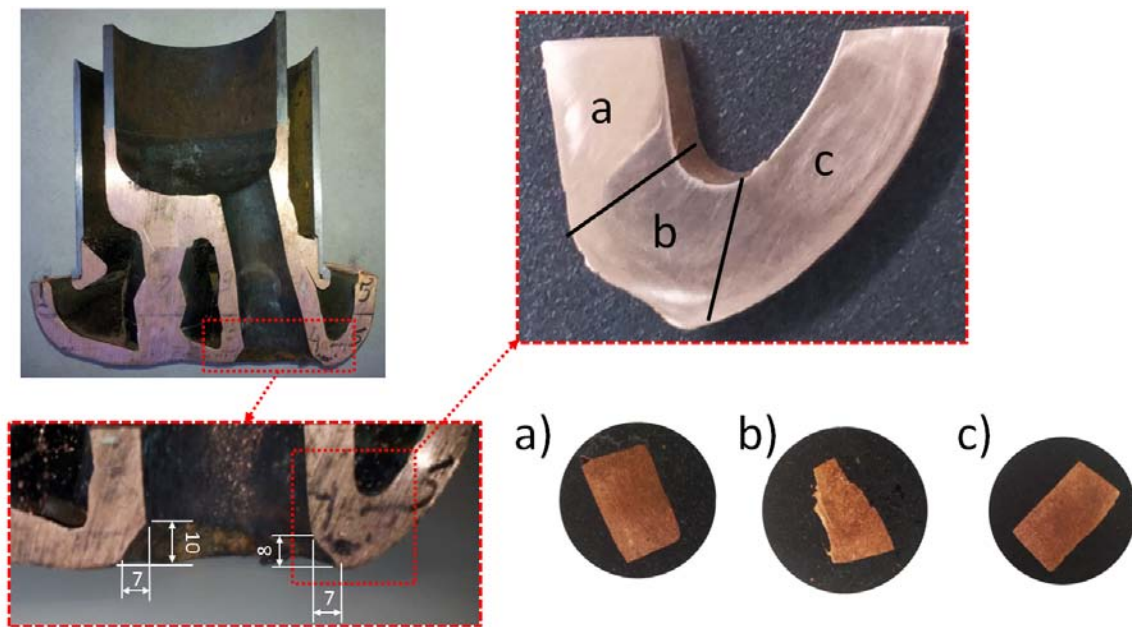


Figure 5: a) Without wear nozzle region; b) Wear region e c) Tip external face.

The samples in Figure 5a and 5b are localized inside the nozzle, where sample 5b referent to wear and 5a an internal part in nozzle without wear. In Figure 5c show a sample of the external face of the tip, region exposed in aggressive environment of the converter. After inlay, is necessary a polishing in appropriate machine and suitable surface treatment. For to reveal grain boundaries, the copper samples were chemical attacked immersion with iron chloride III solution <sup>(7)</sup>.

## 2.2 Geometry and body conditions for the CFD simulation

Checking the supersonic flow of the nozzles, as well as the effects of post-combustion, has a big mathematical complexity because it's a problem that involves compressible flow, chemical reactions with combustion and high temperatures. Thus, its necessary used some model that contains equations for mass, moment and energy balance, turbulence and chemical reactions flowing in a 3D domain.

To solve this problem, was used the commercial software Ansys CFX 15.0, which based in volume finite element method for the transport equations solutions with governing the flow. This method divides the geometry in infinitesimal volumes of control and solves numerically the transport equations for each physical principle. For the prediction of post-combustion reactions in the supersonic jet flow, furthermore the mass and heat transfer, was used Flamelet combustion model, which based in PDF (Probability Density Function) table model. <sup>(8)</sup>

Due to the real operating complexity conditions it's necessary to simplify the domain to be simulated, in a way that allows determining de body conditions and emphasizing the wear in outlet supersonic nozzle. For to reduce the number of elements in the mesh and equations for resolution, was used geometric symmetry of only nozzle and similar methodology presented in Guerra *et al.* (2015) <sup>(9)</sup> and Odenthal (2006) <sup>(10)</sup> articles, shown in figure 6 where was considered 1/15 of the nozzle circumference.

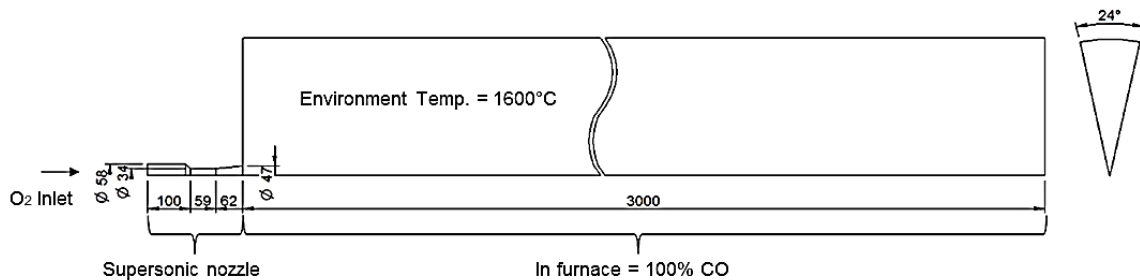


Figure 6: Schematic drawing of the geometry used for CFD simulations.

As the body conditions was considered the O<sub>2</sub> injected through nozzle in a CO external environment, objecting to approximate of converter conditions in decarburization moment. The domain was discretized with 1.005.000 hexahedral mesh elements (Figure 7) and refining in element size near of nozzle, which possibility greater precision in calculates shock wave, flow turbulence and temperature in which is the region of interest.

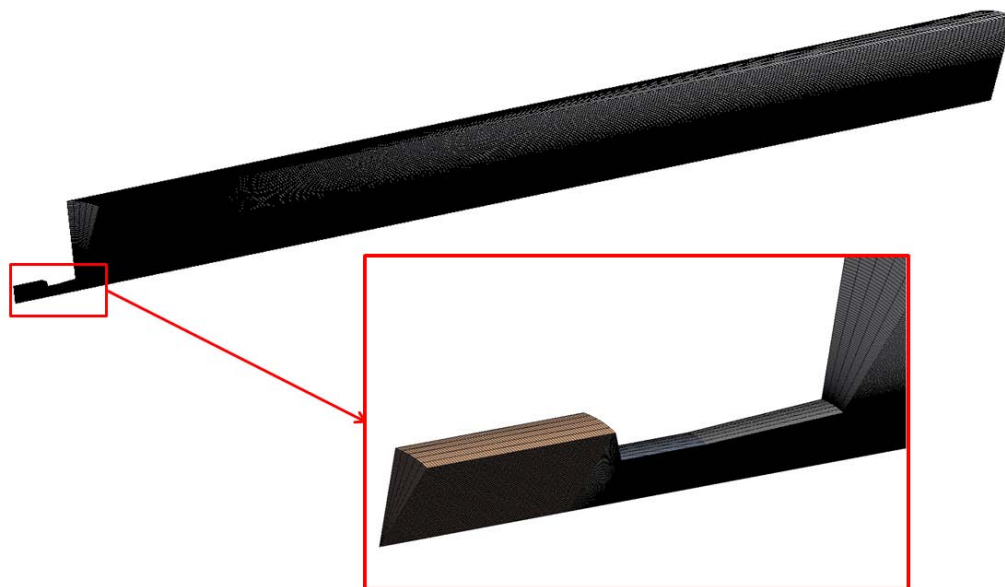


Figure 7: Mesh used in CFD simulation composed for 1.500.000 hexahedral elements.

One of the most relevant factors for wear at the outlet of the nozzles is the oxygen flow <sup>(6)</sup>. In practice, the flow rate may vary around 20% above or below the average flow rate <sup>(5)</sup>, it's considered in CFD simulation. These contour conditions were used both for simulations with the nozzle wear failure geometry, identified as failed nozzle, as for the proposed new geometry, identified as a resized nozzle. In this way, it is expected to verify the effectiveness of the resizing in containing the wear mechanism.

In Table 1 is presented the flow rate, relationship between stagnant and output section area and the nozzle geometry type. The flow rate of 180 Nm<sup>3</sup>/h e 150 Nm<sup>3</sup>/h used in the simulations, refer to the maximum and minimum common flow of the operation, respectively. The only difference between the simulations of the failed and resized nozzle lies in the relation of stagnant and output section area (A/A\*).

Table 1: CFD simulation relationships

|              | Flow rate [m <sup>3</sup> /min] | Relationship A/A* | Environment temp. [°C] | Nozzle type |
|--------------|---------------------------------|-------------------|------------------------|-------------|
| Simulation 1 | 180                             | 1,38              | 1600                   | Failed      |
| Simulation 2 | 150                             | 1,38              | 1600                   | Failed      |
| Simulation 3 | 180                             | 1,15              | 1600                   | resized     |
| Simulation 4 | 150                             | 1,15              | 1600                   | resized     |

The numerical residual used in the simulation is 10<sup>-6</sup>, so the error can't be greater than 0,0001%. Resolution method specified was the High Resolution, for propose less dispersion in the interpolated results.

### 3. RESULTS AND DISCUSSION

#### 3.1 Metallography analysis results

In the Figure 8 is presented the metallography results of the samples showing in Figure 5. It's possible seen in Figure 8a (without wear nozzle region) the granulometric structure remains relatively homogeneous, different from that observed in Figure 8b where is observed a notable grain heterogeneity and its expressive increase compared to the other regions analyzed.

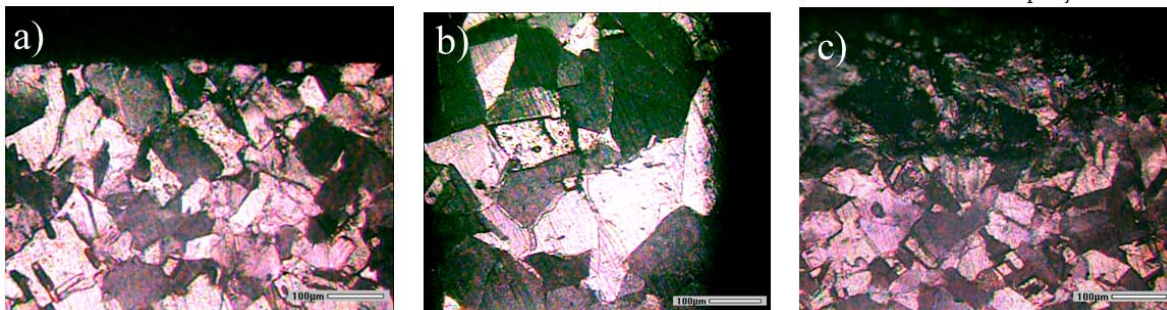


Figure 8: Metallography with magnification of 200X: a) Without wear nozzle region; b) Wear region and c) Tip external face.

The greatest grain growth in the wear region would only be possible if there was a localized thermal input and high temperatures more than found in other regions, based in physical metallurgy principles <sup>(13)</sup>. It is expected to find this disproportionate thermal input in the CFD simulations of the supersonic jet to be presented in the next chapter.

In external tip face (Figure 8c) is observe a same structure verified in the without wear nozzle region. However, in the face exposed at environment the grain have a coalescing characteristic of overheating in short time, which may have been caused for by fusion with liquid metal or slag.

#### 3.2 Simulation results

Is presented in Figure 9 the results in terms of Mach number, which them allows a comparison between the nozzle failed and resize, operating with higher and lower oxygen flow.

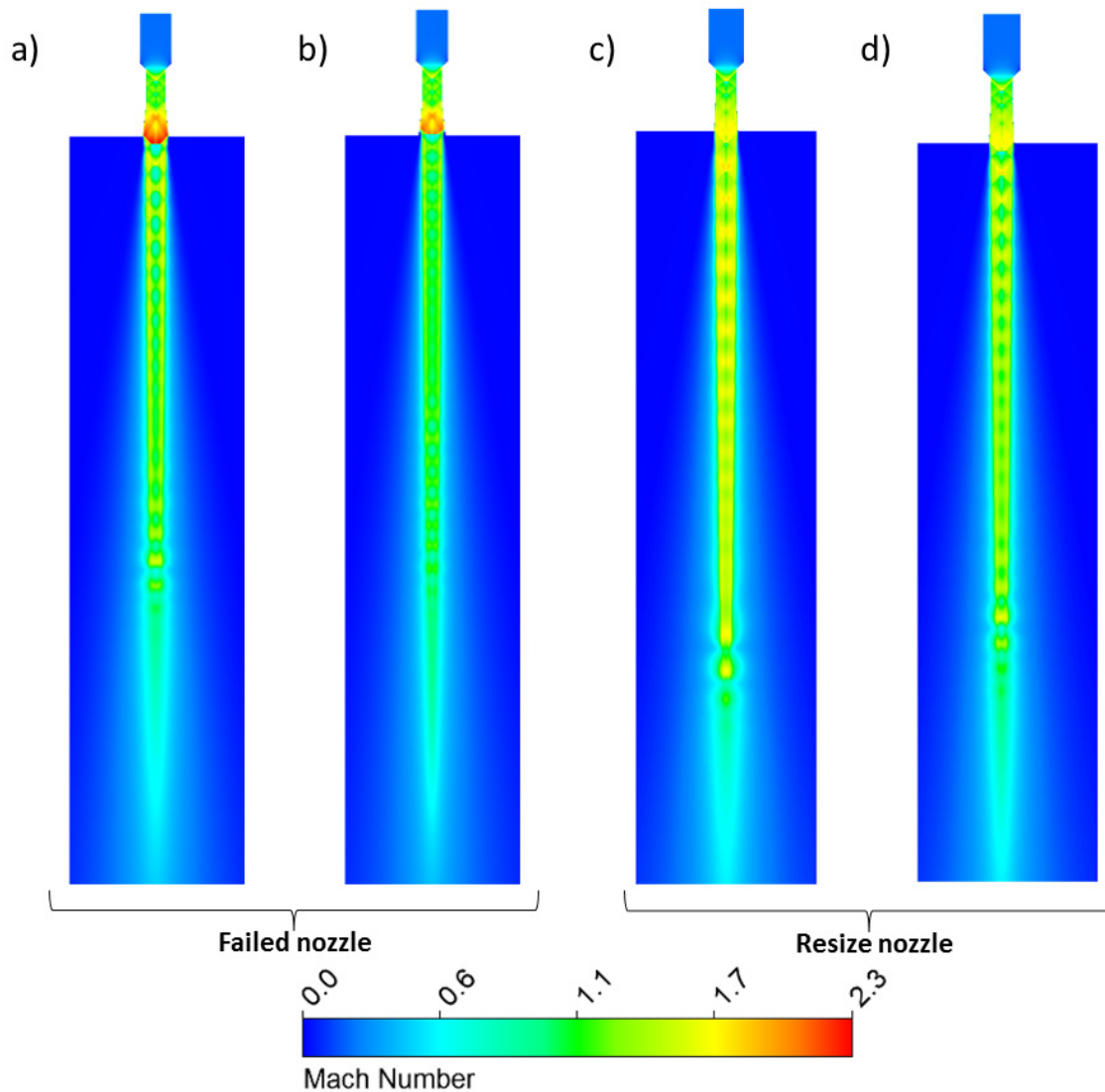


Figure 9: Mach number: a) Simulation 1 (180 m<sup>3</sup>/min); b) Simulation 2 (150 m<sup>3</sup>/min); c) Simulation 3 (180 m<sup>3</sup>/min) e d) Simulation 4(185 m<sup>3</sup>/min).

In the Figure 9a e 9b, higher and lower oxygen flow rate (failed nozzle), verified high intensity shock waves, this prevents the full expansion of the jet out of the nozzle and reduces its effective length. When compare the Figures 9a and 9c, simulations with same flow rate, is possible to verify a considerable increase of potential core of jet in the resized nozzle. It is too observed when compare the Figure 9a e 9c, both with the lower flow rate, where the resizing avoided the formation of the high intensity shock wave at the outlet of the nozzle. This increase of the effective jet core can be better evaluated in Figures 10 and 11.

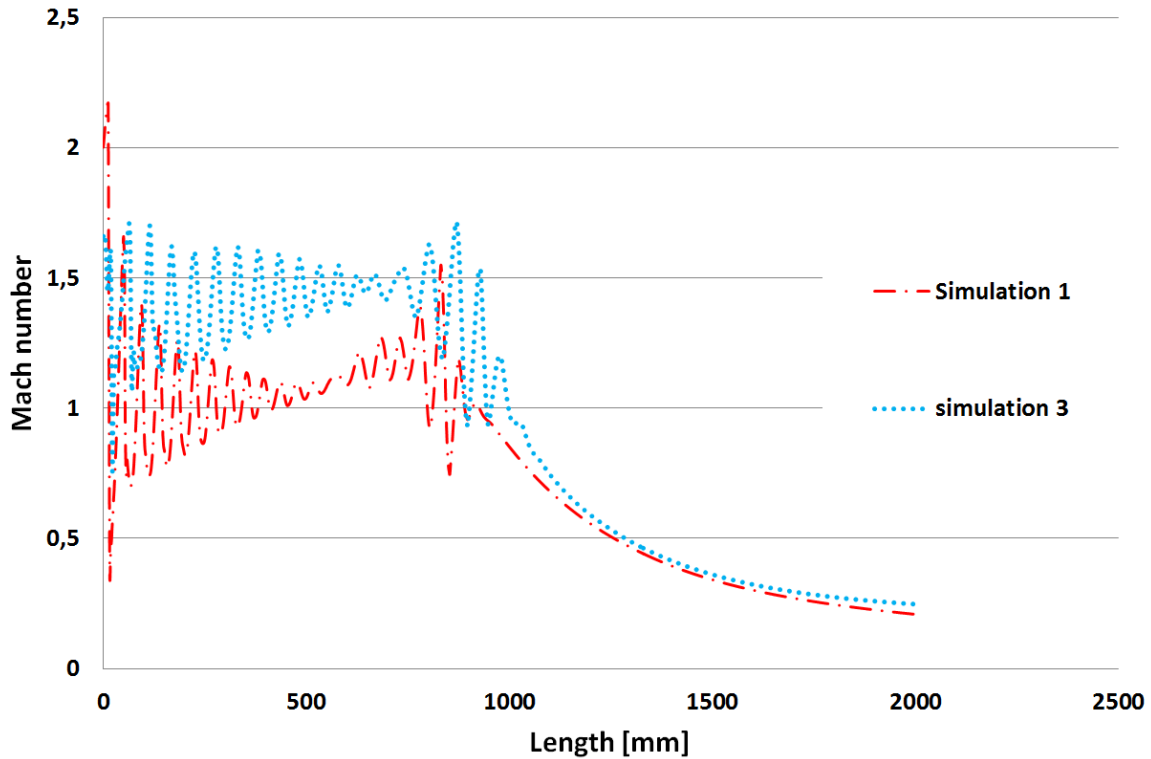


Figure 10: Graph of jet length by Mach number for simulations 1 e 3 (180 m<sup>3</sup>/min).

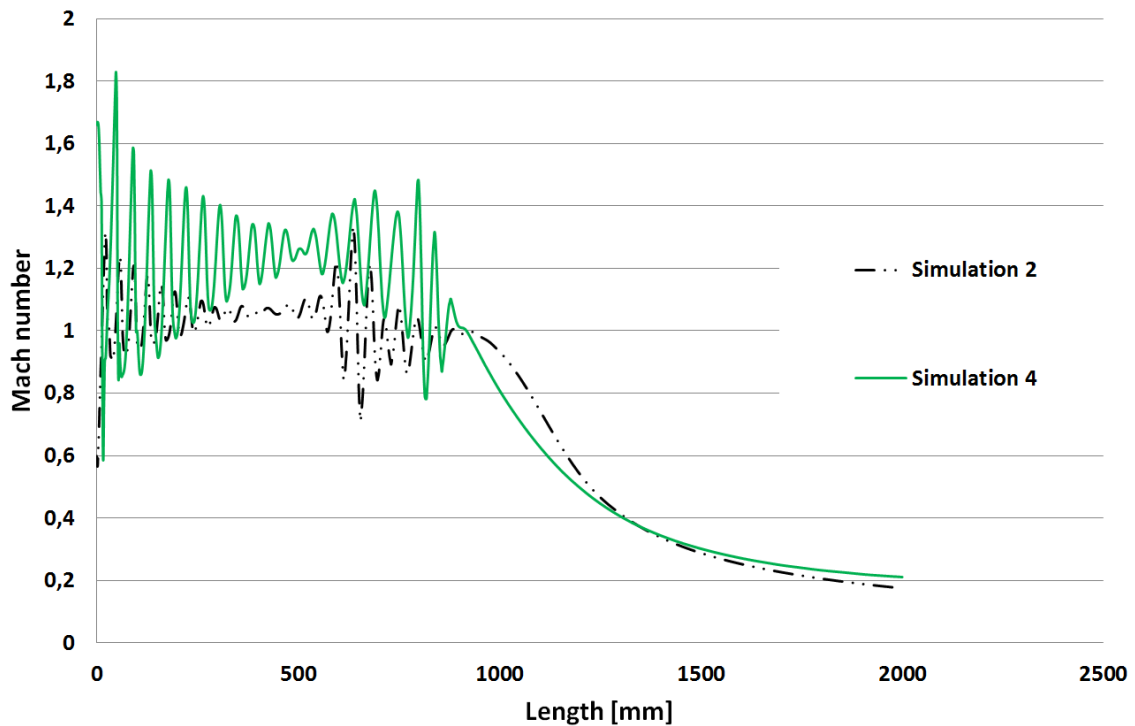


Figure 11: Graph of jet length by Mach number for simulations 1 e 3 (150 m<sup>3</sup>/min).

The gains of the resizing are even more evident when analyzing Figure 12, referring to an magnification near of the nozzles. Is possible seen which besides the high intensity shock wave in Figure 9b occurred detachment of the jet inside the nozzle, but this is not observed in Figure 9d, which has a same body conditions.

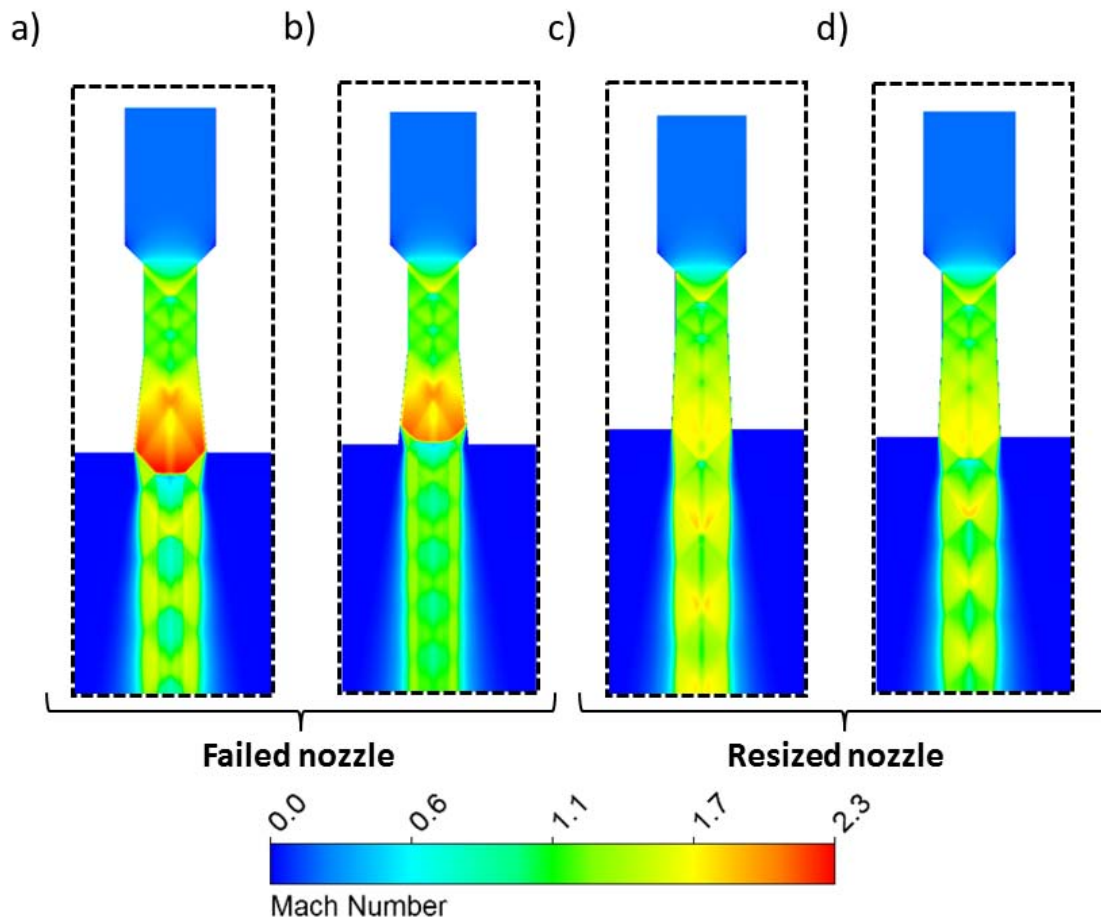


Figure 12: Mach number near outlet nozzle: Simulation 1 (180 m<sup>3</sup>/min); b) Simulation 2 (150 m<sup>3</sup>/min); c) Simulation 3 (180 m<sup>3</sup>/min) e d) Simulation 4 (185 m<sup>3</sup>/min).

The jet detachment happens in function of BOF environment counter pressure, which can compress the jet force the direction of expansion into the nozzle up to a limit, characteristic of shock wave with expansion and compression. Although of the high counter pressure, supersonic speeds still prevail at various points. However, it can propagate through the boundary layer around the jet, since in the near of the boundary layer may vary from supersonic at the interface with the central core and to zero in the wall of the nozzle. Thus, near the walls of the nozzle there are regions with subsonic speeds, generating the jet detachment<sup>(5)</sup>.

The effects of post combustion can be verified in Figure 11 by increase of temperature of 1600 °C (initial body condition) to a level above 3000 ° C. The high temperature around the jet promote an increase the effective core, a same phenomenon presented by Viana & Santos *et al.* (2003)<sup>(13)</sup> in coherent jet injectors.

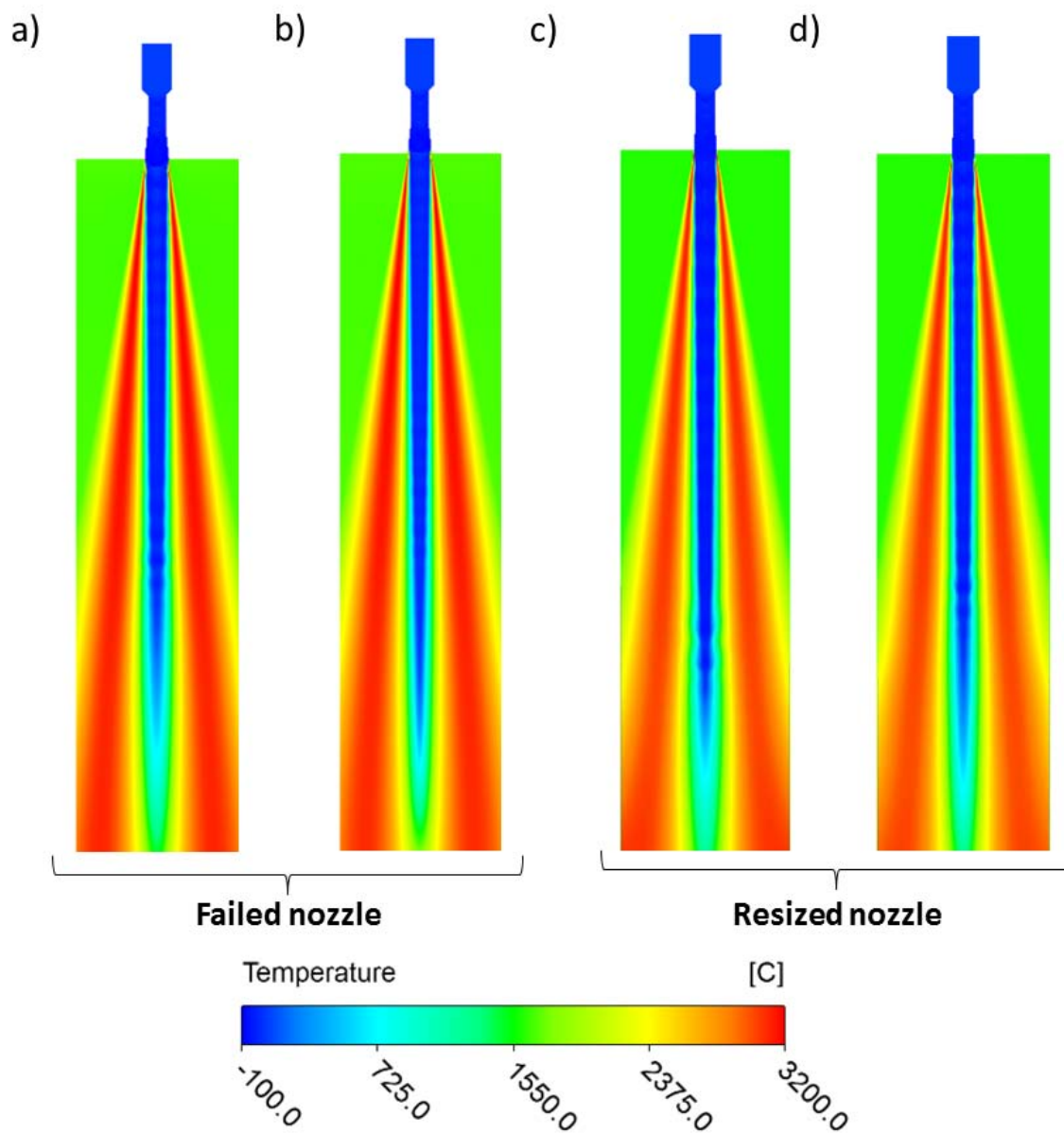


Figure 13: Temperature: a) Simulation 1 (180 m<sup>3</sup>/min); b) Simulation 2 (150 m<sup>3</sup>/min); c) Simulation 3 (180 m<sup>3</sup>/min) e d) Simulation 4 (185 m<sup>3</sup>/min).

The temperature profiles are very similar for all simulations in Figure 11, differentiating itself by the length of the negative temperatures of the potential nucleus, which if shown proportional to the effective core jet length shown in Figure 9. The main differences can be observed near of the nozzle, as shown in Figure 14.

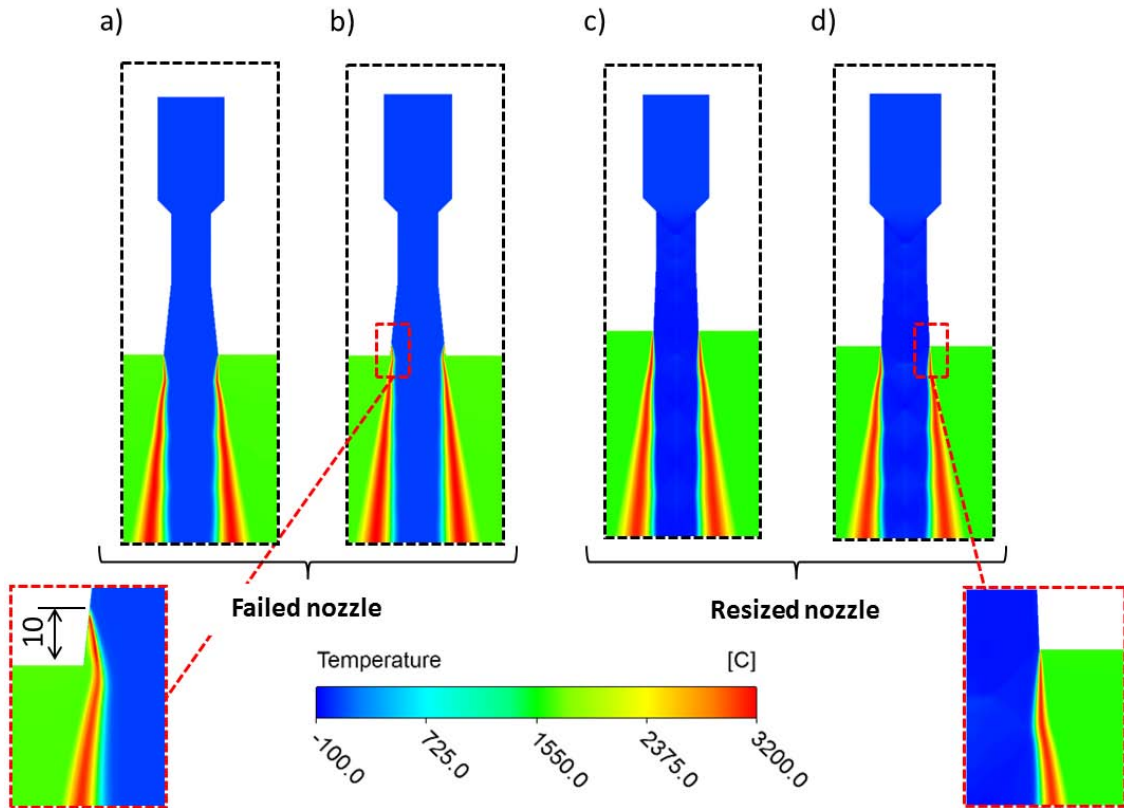


Figure 14: Temperature near of nozzle: a) Simulation 1 (180 m<sup>3</sup>/min); b) Simulation 2 (150 m<sup>3</sup>/min); c) Simulation 3 (180 m<sup>3</sup>/min) e d) Simulation 4 (185 m<sup>3</sup>/min).

It's possible to observe that the detachment provided the initiation of the post combustion inside the nozzle, phenomena verified only in lower flow rate conditions in failed nozzle. In function of jet detachment, are forming pressure negatives zone, which suck the CO from the converter environment into the nozzle, provide the mixing with O<sub>2</sub> in around the jet. The speed flow lines in Figure 15a is consistent with the theory presented by Almqvist (2005) <sup>(14)</sup>.

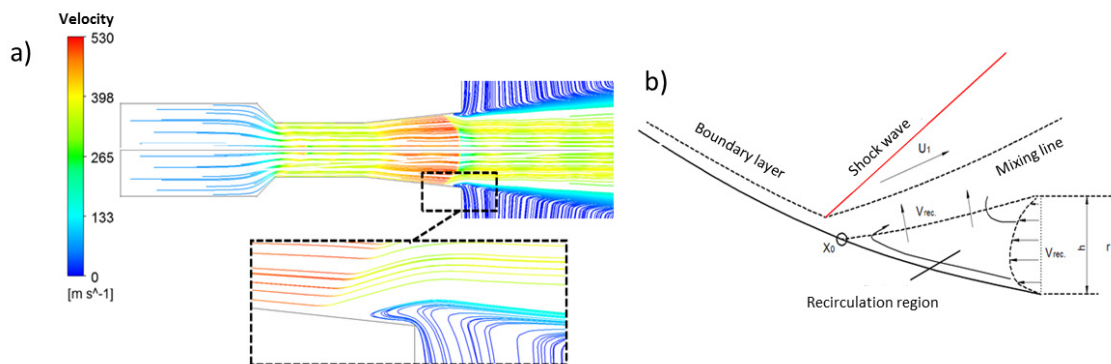


Figure 15: a) Simulation 2: speed flow lines; b) Theoretical flow line when occur detachment jet inside the nozzle. <sup>(14)</sup>

The post combustion inside the nozzle could explain the higher grain growth in the wear region, verified in Figure 8, because it's have a greater thermal input when compared to the other regions. From the flame temperature of 3200 °C concentrated in this region can be estimated through analytical calculations of heat transfer <sup>(15)</sup> that the outlet nozzle the copper reaches with temperatures of approximately 1115 °C, which is above its melting point (1085 °C). Thus, the wear mechanism can be characterized as the gradual melting over the heats. This is because this phenomenon occur only when operating with the lowest operating flow (during measurement with the sub lance), which in this case lasts about 1 min. for heat.

## CONCLUSION

Through the CFD simulations was possible verify which the post combustion of CO have a considerable effect in temperature distribution and supersonic jet flow, reaching flame temperatures above 3000 °C. There was also the occurrence of post-combustion inside the failed nozzle when operating with lower flow rate (150m<sup>3</sup>/min), in function of jet detachment. The thermal input generated by this phenomenon may explain the grain size difference found in the samples, where there was greater grain growth in the region of wear. The jet detachment length inside the nozzle (Figure 14) was also very close to that found in the samples (Figure 8). The working temperature of copper exposed to post-combustion inside the nozzles was estimated at 1115 ° C, being above its melting point of 1085 ° C. Thus, the wear mechanism can be characterized as the gradual melting over the heats, when operating at the lowest operating flow.

Resized nozzle does not have jet detachment, thus it's understood that there will be an increase in the number of heats for if begin or eliminating wear in the nozzles. It's observe also that this which was nozzle resized tendency to increase the effective core jet, due to the more Mach number by length compared with failed nozzle. This provides greater penetration into the bath and, consequently, faster refining reactions.

Thus, it's concluded that CFD simulation tools may be a great aid in the design of supersonic nozzle nozzles of tip lance, because allow considering a greater number of variables of process in the calculations, when compared to analytical methods. Also is that possible to project a nozzle that doesn't wear even with the variations of operational parameters, which are inherent in the steelmaking process.

## ACKNOWLEDGMENT

The authors thank Lumar Metals, Vallourec Brazil and PPGMEC UFMG for the encouragement research. This work is dedicated to the eternal friend of Bruno Orlando Almeida Santos (*in memoriam*).

## REFERENCES

1. Santos, B.O. et al. Simulação Numérica da Vazão de água em Lanças BOF. 45º Seminário de Aciaria - Internacional ABM, Porto Alegre, 25 a 28 maio 2014.
2. Motta, L.S. Análise qualitativa da descarbonização do MRPL da Arcelor Mittal Inox Brasil através do teor de oxigênio do gás da exaustão. UFMG. Belo Horizonte. 2011.
3. White, F.M. Fluid Mechanics. Nova Iorque: McGraw-Hill, 2011. ISBN 978-0-07-352934-9.
4. Zucrow, M.J., & Hoffman, J.D.: *Gas Dynamics* (Vol. I). Toronto: John Wiley & Sons, Inc, 1976.
5. Zuker, R.D., & Biblarz, O.: *Fundamentals of Gas Dynamics* (2ª ed.). California: John Wiley & Sons, 2002.
6. SMS Siemag. Calibration System for Oxygen-Blowing Lances. Düsseldorf, p. 7. 2012.
7. Rohde, R.: *Metalografia e Preparação de Amostras: Uma abordagem prática*. URI, Santo Ângelo, 2010.
8. CFX 15.0. *Solver Theory Guide*. Ansys. USA. 2013.
9. Guerra, M.D., Garajau, F.S., Barros, J.M., & Maia, B.T.: *Desgaste em Bocais de Lança - Simulações CFD e Condições Reais - 46º Seminário de Aciaria Internacional*. Rio de Janeiro, agosto 2015.
10. Odenthal, H.-J., Falkenreck, U., & Schluter, J.: *CFD Simulation of Multiphase Melt Flows in Steel Making Converters*. European Conference on Computational Fluid Dynamics, 2006.
11. Maia, T. *Efeito da Configuração do Bico da Lança na Interação Jato-Banho Metálico em Convertedor*. UFMG. Belo Horizonte, p. 134. 2007.
12. Reed-Hill RE., Abbachian R, Abbachian L: *Physical metallurgy principles*. Stanford: Cengage Learning, 2009.
13. Viana, J. F. et al. *Desenvolvimento do Sopros de Oxigênio com Lança de Jato Coerente na Usiminas*. ABM. São Paulo. 2003.
14. Almqvist, M.: *Semi-empirical Model for supersonic flow separation in rocket nozzle*. Dissertação de mestrado, Departamento de Ciências Espaciais, Kiruna, 2005.
15. Incropera, F.P., Bergman, T.L., Dewitt, D.P. (2008), *Fundamentos de transferência de calor e de massa*, 6ª ed., Editora LTC, Rio de Janeiro-RJ, 643p.

